ENGINEERING RESEARCH JOURNAL (ERJ)
Vol. 1, No. 45 July. 2020, pp. 85 -93
Journal Homepage: http://erj.bu.edu.eg

Nonlinear Analysis of GFRP-Reinforced Concrete Deep Beams

F.B.A. Beshara [1], S.K.S. Elwan [2], Y.M.H. Hammad [1], and E.A.A. Mahmoud [2]
1) Civil Engineering Dept., Faculty of Engineering, Shoubra, Benha University
2) Civil Engineering Dept., Higher Institute of Engineering, El-shrouk Academy, Cairo

Abstract. : In this paper, a non-linear finite element analysis is presented to model the behavior of GFRP-reinforced concrete deep beams with and without web reinforcement. The proposed model that integrates the nonlinear material behavior for concrete and FRP is performed by using the software ANSYS 15. The predicted responses are compared in terms of crack pattern and load deflection relation with experimental results. A good agreement is achieved so the proposed approach is considered a tool for simulating GFRP reinforced concrete deep beams. In addition, parametric studies were carried out to investigate the effect of main structural parameters on the behavior of deep beams. It was drawn that; (1) Increasing the concrete strength, or ratio of flexural reinforcement, or horizontal web reinforcement ratio improves the shear strength and the toughness, (2) Vertical shear reinforcement ratio had insignificant effect on shear strength, and (3) increasing shear span-to-depth ratio reduces the shear strength of deep beam.

Keywords: Reinforced concrete; Deep beams; GFRP; Crack patterns; Load-deflection curves; Shear strength; Finite element; ANSYS.

1. INTRODUCTION

Many steel-reinforced concrete structures, such as bridges, parking garages, and marine structures, are exposed to aggressive environments, which can cause significant damage over time and the need for expensive maintenance due to corrosion of the steel reinforcement. Steel reinforcement corrosion reduces the durability and service life of the structures. An innovative solution to this problem can be applied by using FRP as an alternative to steel reinforcement [1]. FRP bars are excellent corrosion resistance, having high tensile strength and high strength to weight ratio, so FRP bars have been widely used in reinforced concrete members like deep beams.

Deep beams [2] are structural elements, which are used in many structural applications as pile caps, transfer girders, folded plates, tanks, and foundation walls. Deep beams receive single load or a number of small loads and transfer them to a small number of reaction points. Many experimental and theoretical programs have been performed to investigate the behavior of deep beams reinforced with steel bars, e.g. [3-6]. As an alternative to steel bars, some experimental studies were conducted on FRP-reinforced concrete deep beams [7-12]. Also, limited numerical models that have been developed for FRP-RC deep beams, exist in literature [13-17]. In this paper, 3-D Finite Element models, using ANSYS, are proposed to simulate the shear response of GFRP-reinforced concrete deep beams [18]. Based on the good agreement that have been achieved between the numerical predictions and experimental results [10,12], the model was utilized to perform parametric studies to investigate the main parameters effect on behavior of deep beams.

2.Finite Element Modeling of GFRP-Reinforced Concrete Deep Beams

2.1 Finite Element Geometric Idealization

Solid-65 element was used to simulate the geometric discretization of concrete in deep beams. This element is capable of modeling the behavior of reinforced concrete which includes cracking and crushing of concrete in three orthogonal directions, beside the ability to form plastic deformations. In order to overcome stress concentration problems and to avoid localized crushing of concrete elements near the supporting points and applying points, Solid185 was used to simulate the steel plates at support and load locations with thickness 25 mm. Solid-65 and solid185 elements have eight nodal points, each node has three degrees of freedom (translations in the nodal *x*, *y*, and *z* directions) [19] as shown in Figure (1.a) and Figure (1.b), respectively.

Link 180 element is used for modeling the longitudinal and web reinforcement. As shown in Fig. (1-c), it is a 2-node bar linear element. Each node has three degrees of freedom (translations in the nodal x, y, and z directions) [19]. The axial stress is assumed to be uniform over the entire element. The discrete bars are connected to concrete mesh nodes so a perfect bond between the concrete and FRP elements is adopted.

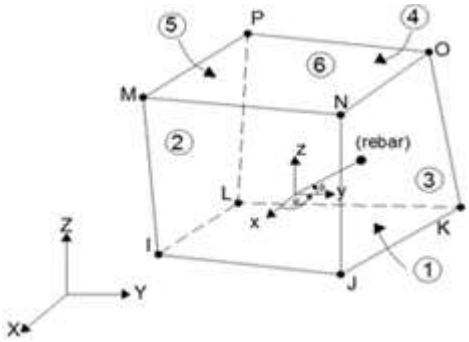

a . Solid 65 Element

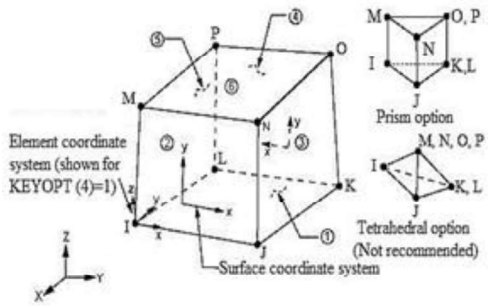

b. Solid 185 Element

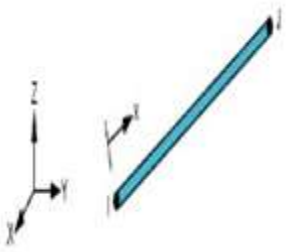

c. link 180 Element

Fig (1) Elements Used for Discretization [19]

2.2 Constitutive Modeling Relations

Various constitutive models were used to model the behavior of concrete in FE simulations of deep beams. In this study, the failure criterion of William and Warnke [20] is employed to simulate the failure surface for concrete in space. Also, the modified model of Hognestad [21,24] is employed to simulate the nonlinear response of concrete in compression. Figure (2) shows the stress-strain curve for concrete in compression. The curve is ascending until the peak stress (fc') and peak strain (ε_o) are reached. It is defined by 7 points. Frist point at 0.3 f_c' and the other points can be calculated based on Equation (1). After reaching the peak stress (f_c') and peak strain (ε_o), (f_c') has a constant value until reaching the value of (ε_{cu}).

$$f_c = f_c'\left[\left(\frac{2\varepsilon_c}{\varepsilon_o}\right) - \left(\frac{\varepsilon_c}{\varepsilon_o}\right)^2\right] \quad 0 \le \varepsilon_c < \varepsilon_o \qquad (1)$$

$$\varepsilon_o = \frac{2f_c'}{E_c} \qquad (2)$$

Where: f_c = the compressive stress in the principal *i*-direction, ε_c = the compressive strain in the principal *i*-direction, E_c = the initial tangent modulus for concrete in MPa, and is defined according to ACI 318 -18 [22] by the following equation:

$$E_c = 4700\sqrt{f_c'} \qquad \text{(MPa)} \qquad \text{....(3)}$$

Figure (3) illustrates the stress strain curve for concrete in tension [23]. At first, the curve is ascending in which the constitutive relationship is assumed to be linear till reaching the tensile strength of concrete. The ascending branch is defined by the peak tensile strength (f_t) and modulus of elasticity (E_c). The corresponding strain (ε_{cr}) to the peak stress which indicates the appearance of the crack initiation. After crack initiation, the behavior of discontinuous macro-cracks is presented by a smeared model so, the concrete tensile stress is dropped by 40% of the peak tensile strength (f_t). The rest of the model is represented as the curve that descends linearly to zero tensile.

$$f = E_t\,\varepsilon_t \qquad 0 \le \varepsilon_t \le \varepsilon_{cr} \tag{4}$$

$$f_t = E_t\,\varepsilon_{cr} \tag{5}$$

$$f = \mathrm{T}_c\, f_t \left[\frac{\varepsilon_b - \varepsilon_t}{\varepsilon_b - \varepsilon_{cr}}\right]$$

$$\varepsilon_{cr} \le \varepsilon_t \le \varepsilon_b \tag{6}$$

Where: f_t is uniaxial tensile cracking stress (f_t = 0.1 f_c`), Tc is a multiplier for amount of tensile stress relaxation (defaults to 0.6), ε_{cr} is uniaxial tensile cracking strain (ε_{cr} = 0.1 ε_0). ε_b is the maximum tensile strain for cracked concrete is given by six times the cracking strain ε_{cr} ($\varepsilon_b = 6\,\varepsilon_{cr}$).

A shear transfer coefficient β_t, is introduced which represents a shear strength reduction factor for cracked concrete. Typical shear transfers coefficient ranges from 0.0 to 1.0, where zero-value indicates a very smooth crack (complete loss of shear transfer) and 1.0 value indicates a very rough crack (no loss of shear transfer). Shear transfer coefficients are taken as 0.1 for open crack and 0.9 for closed crack. A value of 0.6 for stress relaxation after cracking was taken in analysis. These values showed better behavior for selected specimens according to the experimental studies, which have been used.

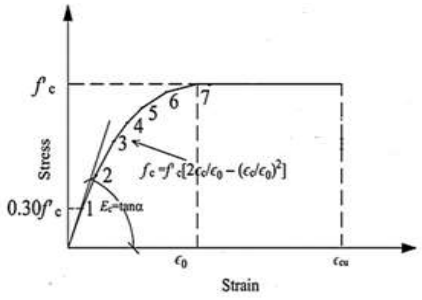

Fig (2) Stress-Strain Curve of Concrete in Compression [24]

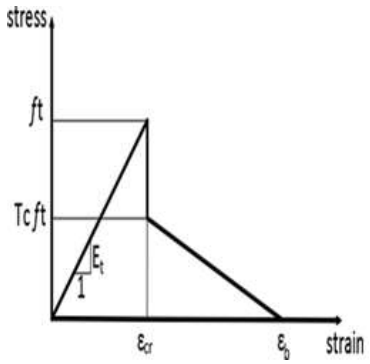

Figure (3) Stress-Strain Curve of Concrete in Tension [23]

Figure (4) shows the stress-strain curve of the FRP bars embedded in concrete, which is adopted [1] in the simulation of both web and longitudinal reinforcement bars of the specimens. This behavior is identical in tension and compression. The FRP bars are simulated as elastic-brittle materials until rupture. At the ultimate, the stress and strain are given by f_{fu} and ε_{fu}, respectively. The elasticity modulus of FRP is given by E_{FRP}.

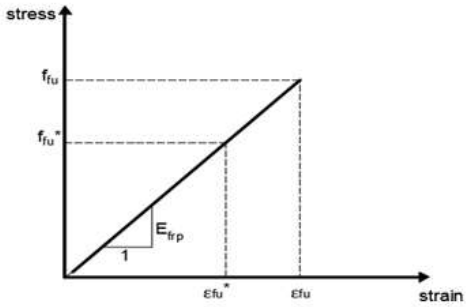

Fig (4) Stress-Strain Curve for FRP Bars [1]

$$f_{fu} = E_{FRP} * \varepsilon_{fu} \tag{7}$$

Where; f_{fu} is the ultimate tensile strength, ε_{fu} is the ultimate ruptures strain and E_{FRP} is the tensile modulus of elasticity of FRP bars.

3.Validation Studies

3.1 Model Description of the Selected Deep Beams

Several concrete deep beams were selected [18] for validating the results of analysis using ANSYS 15. Only, two case studies are mentioned here. In the first case study, GFRP-reinforced concrete deep beam without web reinforcement (G8N6) was selected, and experimentally tested in [12]. For deep beam (G8N6), GFRP longitudinal reinforcement ratio ρ% was 0.69%, ultimate tensile strength f_{frp} was 790 MPa and E_{FRP} modulus of elasticity was 47.6 GPa. The concrete compressive strength (f_c'), concrete tensile strength (f_t) and young's modules (E_c) were respectively 49.3 MPa, 4.6 MPa and 33 GPa. In the second case study, GFRP-reinforced concrete deep beam with web reinforcement (G1.13VH) was chosen and experimentally tested in [10]. For deep beam (G1.13VH), the concrete compressive strength (f_c'), concrete tensile strength (f_t) and young's modules (E_c) were respectively 37 MPa, 3.4 MPa and 28.6 GPa. GFRP longitudinal reinforcement ratio ρ% was 1.21%, ultimate tensile strength f_{frp} was 1000MPa and modulus of elasticity E_{FRP} was 66.4GPa. GFRP vertical web reinforcement ratio ρ_v% was 0.42%, ultimate tensile strength f_{frp} was 1312 MPa and modulus of elasticity E_{FRP} was 65.6 GPa.

GFRP horizontal web reinforcement ratio ρ_h% was 0.68%, ultimate tensile strength f_{frp} was 1184 MPa and modulus of elasticity E_{FRP} was 62.6 GPa. The typical dimensions and reinforcement configurations of the deep beams are shown in Figure (5).

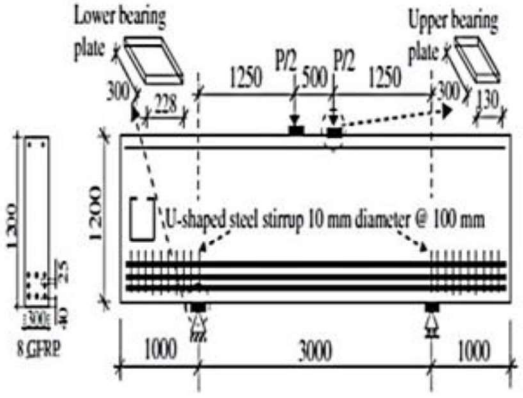

a .Deep Beam (G8N6)[12]

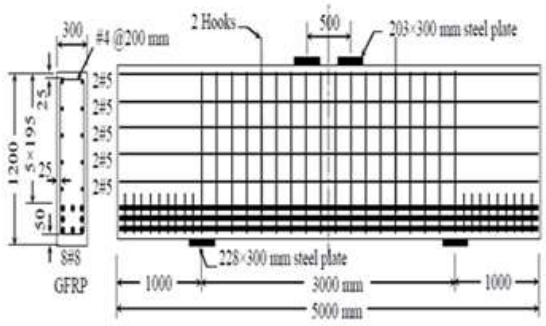

b. Deep Beam (G1.13VH) [10]

Fig (5) Typical Dimensions and Reinforcement Configurations of Deep Beams

Figure (6) and Figure (7) show the 3-D finite element simulation models and present GFRP reinforcement configuration for the two beams. The type of mesh used in the beam model is hexahedron (brick) structured element with density (100×100×100) to obtain good results.

The GFRP longitudinal and web reinforcement are modeled by LINK180 element at the nodes created from the meshing. The plates are modeled by SOILD185 element with thickness 25 mm to prevent the stress concentration. The Poison's ratio is considered to be 0.2 and 0.3 for concrete and steel plates, respectively.

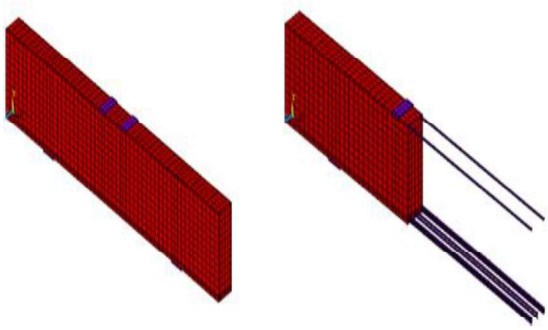

Fig (6) Finite Element Model for Deep Beam (G8N6)

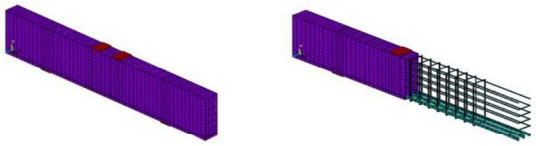

Fig (7) Finite Element Model for Deep Beam (G1.13VH)

To constrain the model, one support is simulated as hinged support in which the translations at the nodes are equal to zero while the other support is simulated as roller support in which the vertical translations at the nodes are equal to zero. In order to simulate the experimentally tested deep beams, the displacement is applied on the loading plate in the gravity direction. The displacement is applied as incremental loads. The displacement increment was set at 1% of the experimental maximum displacement. The maximum number of iterations was set to 100 in each load step and the equilibrium tolerance of 3% was chosen.

3.2 Predicted Load-Deflection Curves

To validate the proposed FE model, the numerical and experimental load-deflection curves are compared in Figure (8). Based on load-deflection curve, the ultimate load carrying capacity (P_u) and the corresponding ultimate deflection (Δ_u) can be obtained. The specimens exhibited a nearly bilinear response up to failure. The following results can be concluded from the figure; (1) At the ultimate level, the numerical predictions are close to the experimental results, (2) The ratio [($P_{u,(EXP)}$) / $P_{u,(FE)}$] for (G8N6) and (G1.13VH) is 0.89 and 1.01 respectively, (3) The ratio between the corresponding deflection [($\Delta_{u\ (EXP.)}$)/ ($\Delta_{u\ (FE)}$)] for (G8N6) and (G1.13VH) is 0.97 and 1.1 respectively, and (4) The toughness ratio [$I_{(EXP)}$/$I_{(FE)}$] for (G8N6) and (G1.13VH) is 0.94 and 1.07 respectively.

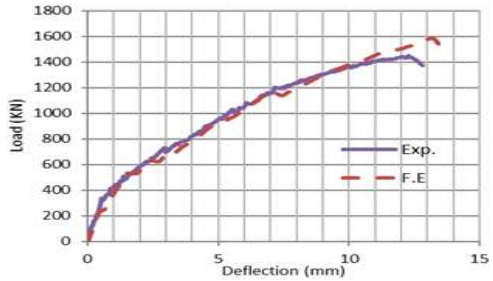

a. Deep Beam (G8N6)

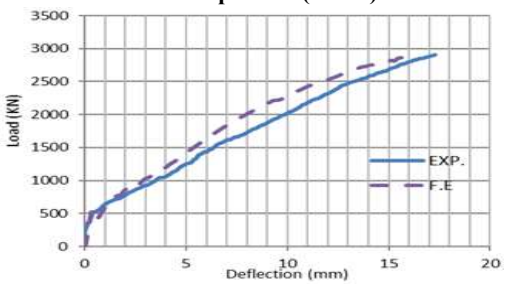

b. Deep Beam (G1.13VH)

Fig (8) Load-Deflection Curves for Deep Beams

3.3 Predicted Failure Mode and Cracking Patterns

As shown in Figure (9), the predicted crack patterns are compared with the experimental crack patterns [10,12], so good agreement is noticed. The failure of the specimens was brittle, where diagonal shear failure of concrete is the predicted failure mode for the specimens.

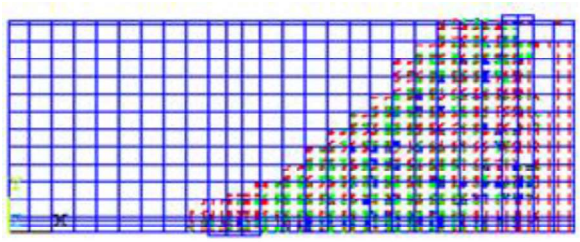

a. Predicted Crack Pattern for (G8N6)

b. Exp. Crack Pattern for (G8N6)

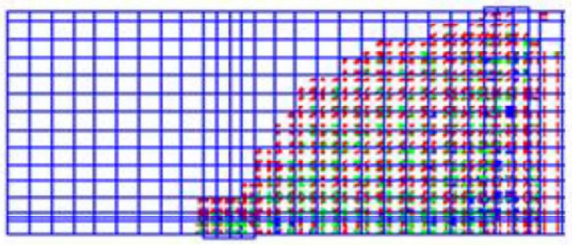

c. Predicted Crack Pattern for (G1.13VH)

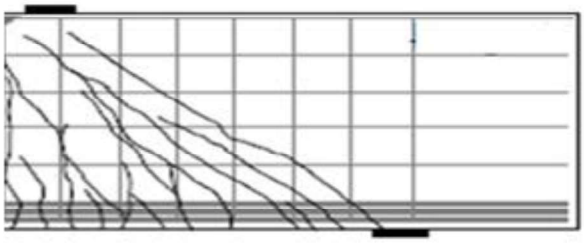

d. Exp. Crack Pattern for (G1.13VH)

Fig (9) Cracking Patterns for the predicted and observed results

4.Parametric Studies

A series of FRP-reinforced concrete deep beams specimens, which have been numbered with (S1,S2,S3,…..S15) are analyzed to investigate the influence of different parameters. The main parameters are listed in Table (1), which includes: (1) shear span-to-depth ratio (a/d) (2) the concrete strength (f_c`), (3) ratio of main reinforcement (ρ%), (4) ratio of horizontal shear reinforcement (ρ_h%), and (5) ratio of vertical shear reinforcement (ρ_v%). For each parameter, the predicted load-deflection curve is plotted. (G8N6) [12] is taken as a reference specimen used in parametric study.

Table (1): The Input Parameters for the Studied Specimens

Deep Beam	*a/d*	f_c` *(MPa)*	*ρ %*	ρ_h %	ρ_v %	*Studied Parameter*
S1	**0.83**	49.3	0.69	---	---	*a/d*
S2	**1.13**	49.3	0.69	---	---	
S3	**1.47**	49.3	0.69	---	---	
S4	1.13	**40**	0.69	---	---	*fc'*
S5	1.13	**49.3**	0.69	---	---	
S6	1.13	**60**	0.69	---	---	
S7	1.13	49.3	**0.48**	---	---	ρ %
S8	1.13	49.3	**0.69**	---	---	
S9	1.13	49.3	**1.23**	---	---	
S10	1.13	49.3	0.69	---	---	ρ_h %
S11	1.13	49.3	0.69	**0.15**	---	
S12	1.13	49.3	0.69	**0.47**	---	
S13	1.13	49.3	0.69	---	---	ρ_v %
S14	1.13	49.3	0.69	---	**0.25**	
S15	1.13	49.3	0.69	---	**0.42**	

4.1 Effect of Shear Span-to-Depth Ratio (a/d)

The behavior of three GFRP-reinforced concrete deep beams are studied with different values of shear span - to-depth ratio (a/d) .The specimens S1,S2 and S3 are modeled using (a/d) ratios (0.83,1.13 and 1.47) respectively. Figure (10) illustrated the predicted load-deflection curves for these specimens. It is obvious that shear span-to-depth ratio has a significant effect on the shear behavior of deep beams. By decreasing (a/d) ratio, the ultimate shear capacity of the deep beams tended to increase while the value of the mid span deflection decreases. For specimens S2 and S3, (a/d) ratio increased by 36% and 77% respectively and (P_u) decreased by 41.8 % and 92.7% respectively when compared to S1. In addition, the increase of (a/d) enhances the mid span deflection for specimens S2 and S3 by 55% and 124% respectively when compared to S1.

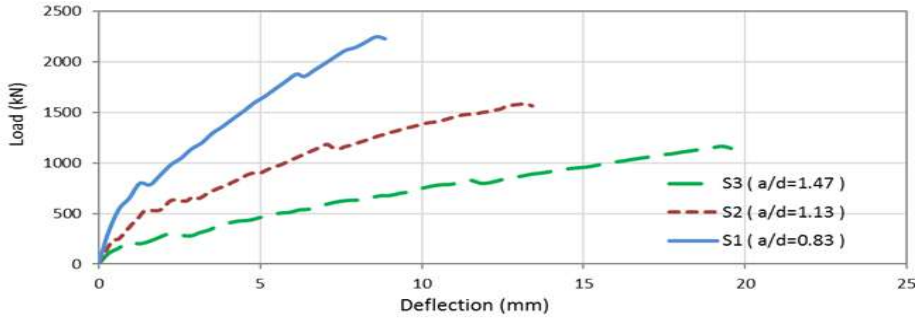

Fig (10) Predicted Load-Deflection Curves for Deep Beams S1, S2 and S3

4.2 Effect of Concrete Compressive Strength (f_c')

Figure (11) presented the predicted load-deflection curves for three deep beams with various value of concrete compressive strength. The specimens are donated by S4, S5 and S6 with different (f_c') values as 40, 49.3 and 60 MPa, respectively. The comparison between the results clarified that the increasing in (f_c') improves the predicted ultimate shear capacity for specimens S5 and S6 by 25% and 57.5% respectively when compared to S4. In addition, there is enhancement in toughness (I) by 40 % and 112% for specimens S5 and S6 when compared to S4.

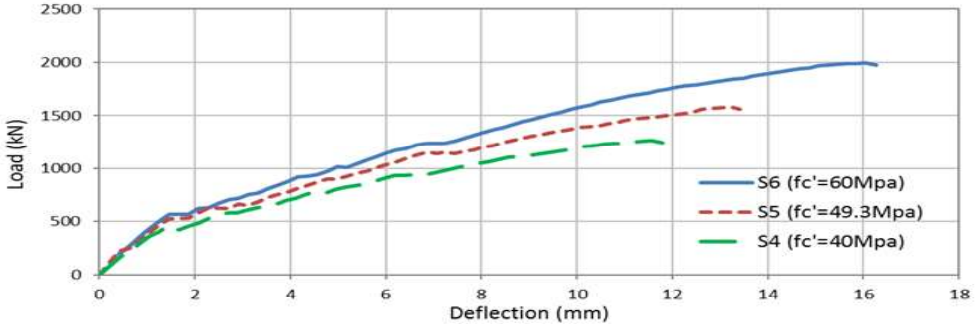

Fig (11) Predicted Load-Deflection Curves for Deep Beams S4, S5 and S6

4.3 Effect of Flexural Reinforcement Ratio (ρ %)

Three GFRP-reinforced concrete deep beams with different ratio of flexural reinforcement, were studied, and referred as S7,S8 and S9. The analyzed specimens were reinforced with (ρ %) as 0.48%,0.69% and1.23% respectively. The predicted load-deflection curves are plotted in Figure (12). An improvement in the predicted ultimate shear capacity is noticed as the flexural reinforcement ratio increased. When (ρ%) increased from 0.48% to 0.69%, (P_u) increased by 32.5%. however, when (ρ%) increased from 0.48% to 1.23%, (P_u) increased by 82.6%. The toughness ratio for S8 and S9 are increased by 64% and 181.7% respectively when compared to S7.

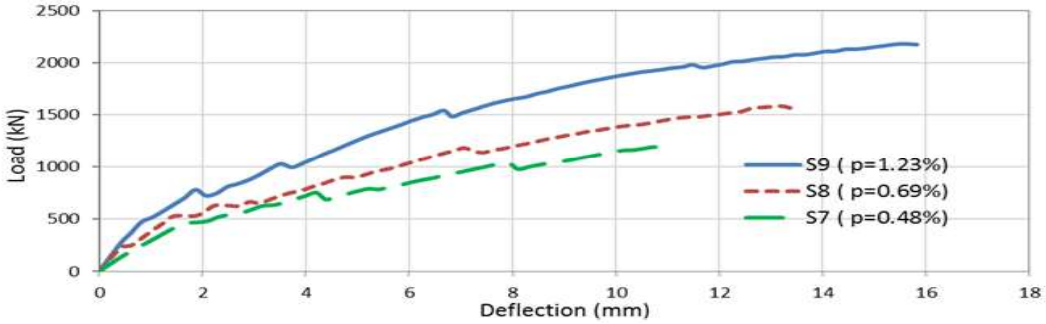

Fig (12) Predicted Load-Deflection Curves for Deep Beams S7, S8 and S9

4.4 Effect of Horizontal Shear Reinforcement Ratio (ρ_h%)

Figure (13) presented the load-deflection curves for the three GFRP-reinforced concrete deep beams with different ratio of horizontal shear reinforcement. The specimens are defined by S10, S11 and S12 with (ρ_h%) 0%, 0.15% and 0.47% respectively. An enhancement in ultimate shear capacity is predicted for specimens S11 and S12 by 11.5% and 23% respectively when compared to S10.The toughness ratio increases by 20% and 45% for S11 and S12 respectively when compared to S10. By increasing the (ρ_h%), the mid-span deflection decreased at the same applied load.

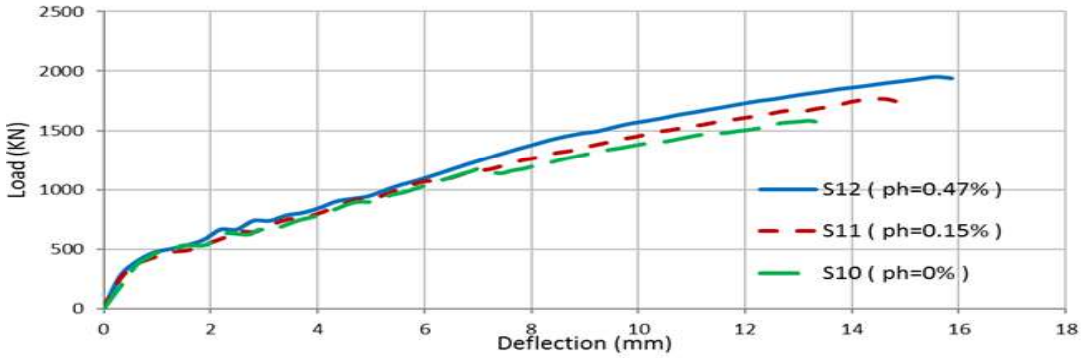

Fig (13) Predicted Load-Deflection Curves for Deep Beams S10, S11 and S12

4.5 Effect of Vertical Shear Reinforcement Ratio (ρ_v%)

Three GFRP concrete deep beams with different ratio of vertical reinforcement are modeled. The studied ratios of vertical shear reinforcement are 0% , 0.25% and 0.42% for specimens S13,S14 and S15 respectively. According to load-deflection curve for specimens; shown in Figure (14), the (ρ_v%) has an insignificant effect on ultimate shear capacity. The shear capacity increased by 1.3% ,when (ρ_v%) increased from 0% to 0.42%.On the other hand, the deflection at ultimate load decreased by 15.5% when (ρ_v%) increased from 0% to 0.42% as shown in Figure (14).

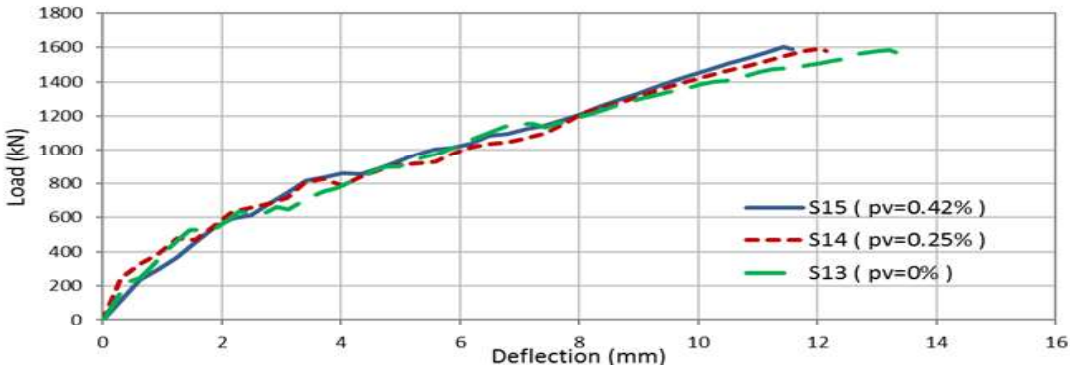

Fig (14) Predicted Load-Deflection Curves for Deep Beams S13, S14 and S15

5. Conclusions

In this paper, the nonlinear finite element program ANSYS was used to predict the behaviour and strength of GFRP-reinforced concrete deep beam with and without web reinforcement. From the validation and the parametric studies, the following conclusive points are drawn:

1) For all case studies, the results from the predicted model simulate a good agreement with experimental results in terms of the load-deflection response, the cracking patterns and the failure modes. The overall average for [$P_{u, EXP}$/ $P_{u, FE}$] ratio, [$\Delta_{u, EXP}$/ $\Delta_{u, FE}$] ratio and [I_{EXP}/ I_{FE}] for all specimens are 0.95, 1.03 and 1.01 respectively. This indicates the suitability of the proposed numerical technique for nonlinear analysis of GFRP-reinforced concrete deep beams.
2) Increasing the shear span-to-depth ratio (*a/d*) reduces the ultimate shear capacity. Using deep beams with (*a/d*) = 1.13 and 1.47 decreases the load capacity by 41.8 % and 92.7%, respectively, and increases the mid-span deflection by 55% and 124%, respectively when compared to deep beam with (*a/d*) = 0.83.
3) An improvement in the ultimate shear capacity is noticed as the flexural reinforcement ratio (ρ%), or concrete strength (f_c`) is increased. The increase of (ρ%) from 0.48% to 0.69% & 1.23%, increases ($P_u$) by 32.5% & 82.6%, respectively. Compared to deep beam with $f_c$` = 40 MPa, the use of fc`= 49.3 MPa & 60 MPa, shear capacity is increased by 25% & 57.5% respectively.

4) Vertical web reinforcement has insignificant effect on the ultimate shear capacity of deep beams reinforced with GFRP bars. Decreasing in deflection clarifies the effectiveness of vertical bars to control crack width.
5) The minimum horizontal shear reinforcement ratio (ρ_h%) improved the ultimate shear capacity by 11.5%, compared with deep beams without horizontal reinforcement. The horizontal shear reinforcement is more effective than vertical on ultimate shear capacity.

References

[1] Design Manual No.3, "Reinforcing Concrete Structures with Fiber Reinforced Polymers", The Canadian Network of Centers of Excellence on Intelligent Sensing for Innovative Structures, ISIS Canada Corporation, Winnipeg, Manitoba, Canada (2006).

[2] Egyptian Code of Practice ECP 203, "Design and Construction of Reinforced Concrete Structures", Ministry of Building and Construction, 2018.

[3] Tuchscherer, R.," Distribution of Stirrups Across Web of Deep Beams", ACI Structural Journal, Vol.95, No.4, Nov.2011, pp.378-401.

[4] Lu, W., Y., Lin, I., J., and Yu, H., W.," Shear Strength of Reinforced Concrete Deep Beams ", ACI Structural Journal, Vol.110, No.4, Jul.-Aug. 2013, pp.268-282.

[5] Moran, J. D., and Lubell, A.," Behavior of Deep Beams Containing High-Strength Longitudinal Reinforcement", ACI Structural Journal, Vol.113, No.1, Jun.-Feb.2016, pp.142-156.

[6] Zhang, J. H., Li, S.S., Xie, W., and Guo, Y. D.," Experimental Study on Shear Capacity of High Strength Reinforcement Concrete Deep Beams with Small Shear Span–Depth Ratio", Materials journal, Vol.1218, No.13, Mar. 2020.

[7] El-Sayed, A., El-Salakawy, E., and Benmokrane, B.," Shear Strength of Fiber-Reinforced Polymer Reinforced Concrete Deep Beams Without Web Reinforcement", NRC Research Press, Vol.39, No.1, Apr.2012, pp. 546–555.

[8] Abed, F., El-Chabib, H., and Alhamaydeh, M.," Shear Characteristics of GFRP-Reinforced Concrete Deep Beams without Web Reinforcement", Journal of Reinforced Plastics and Composites, Sep.2012, pp. 1063-1073.

[9] Andermatt, M., and Lubell, A.," Behavior of Concrete Deep Beams Reinforced with Internal Fiber-Reinforced Polymer ", ACI Structural Journal, V. 110, No. 4, Jul.-Aug. 2013, pp.595-605.

[10] Mohamed, K., Farghaly, A. S., and Benmokrane, B.," Effect of Web Reinforcement in FRP-Reinforced Deep Beams ", The 7th International Conference on FRP Composites in Civil Engineering, Canada, Aug.2014.

[11] Issa, M., Issa, H., and Sherif, E.," Behavior and Modeling of Concrete Deep Beams Reinforced with GFRP Rebars ", 1st International Conference on Innovative Building Materials, Fayoum University, Egypt, Dec.2014.

[12] Farghaly, A.S., and Benmokrane, B.," Shear Behavior of FRP-Reinforced Concrete Deep Beams without Web Reinforcement," Journal of Composites for Construction, Vol. 10, Apr.2013.

[13] Abed, F., and Al-Rahmani, A.," Finite Element Simulations of The Shear Capacity Of GFRP-Reinforced Concrete Short Beams, "IEEE ", Vol. 9, No. 13, Nov.2013, pp. 4673-5814.

[14] Metwally, I.," Nonlinear Analysis of Concrete Deep Beam Reinforced With GFRP Bars Using Finite Element Method ", Malaysian Journal of Civil Engineering, Vol.26, No.2, Sep.2014, pp. 224-250.

[15] Mohamed, K., Farghaly, A. S., Benmokrane, B., and Neale, K.," Nonlinear Finite-Element Analysis for The Behavior Prediction and Strut Efficiency Factor of GFRP-Reinforced Concrete Deep Beams", Engineering Structures, Vol.137, No.1, Feb.2017, pp. 145–161.

[16] Markou, G., and AlHamaydeh, M.,"3D Finite Element Modeling of GFRP-Reinforced Concrete Deep Beams without Shear Reinforcement", International Journal of Computational Methods, Vol 15, No. 2, 1-35, Mar.2017.

[17] Salman ,W., "Nonlinear Behavior of Reinforced Concrete Deep Beams Reinforced with Internal Fiber-Reinforced Polymer", International Journal of Civil Engineering and Technology, V. 9, No. 11, Nov.2018, pp. 2811–2825.

[18] Mahmoud, E.A.A.," Shear Response of FRP- Reinforced Concrete Deep Beams", M.Sc. Thesis to be Submitted, Benha University, Faculty of Engineering, Shoubra, Egypt, 2020.

[19] ANSYS Inc., "ANSYS Mechanical APDL Theory Reference: Release 15.0", Canonsburg PA, USA, 214

[20] Willam, K. J., and Warnke, E. P., "Constitutive Model for Triaxial Behavior of Concrete," Seminar on Concrete Structures Subjected to Triaxial Stresses, International Association of Bridge and Structural Engineering Conference, Bergamo, Italy, 1974, 174 pp.

[21] Hognestad, E. "A Study on Combined Bending and Axial Load in Reinforced Concrete Members." Univ. of Illinois Engineering Experiment Station, Univ. of Illinois at Urbana-Champaign, IL, 1951, 43-46.

[22] ACI Committee 318, "Building Code Requirements for Structural Concrete (ACI 318-18) and Commentary (ACI 318-R-18)", ACI, Farmington Hills, 2018.

[23] Park R., Paulay T., “Reinforced Concrete Structures”, New York: John Wiley & Sons; 1975.

[24] Jnaid,F. and Aboutaha,R.," Residual Flexural Strength of Reinforced Concrete Beams with Unbonded Reinforcement", ACI Structural Journal, V. 111, No.6, Jan.-Dec. (2014), 1-15.